Proceedings of the National Academy of Sciences, India Section A: Physical Sciences
https://doi.org/10.1007/s40010-024-00882-y

SCIENTIFIC RESEARCH PAPER

Effect of Polyvinylpyrrolidone on Antioxidant and Antibacterial Activity of Silver Metal Nanoparticles: A Comparative Analysis

B. Dinesh[1] · Jagadeesha Poyya[1,2] · Farhan Zameer[3] · Lokesh Koodlur Sannegowda[4] · Chandrashekhar G. Joshi[1] · Anjanapura V. Raghu[5,6]

Received: 2 December 2022 / Revised: 17 April 2024 / Accepted: 29 May 2024

Abstract
Nanotechnology research has advanced in the past two decades because of its tunable physicochemical properties. Among the wide range of metal-based nanoparticles, silver nanoparticles (AgNPs) have gained intense research prominence because of their peerless features such as excellent electrical conductivity, catalysis, and a broad range of promising bioactivities such as antioxidant, antibacterial, antifungal, anti-inflammatory, and anticancer effects. In attaining the colloidal stability of silver nanoparticles, capping plays an important role. These capping compounds are believed to provide dual functionality in the synthesis process, acting both as structure-directing and stabilizing agents. Polyvinylpyrrolidone (PVP) is a biocompatible, *p*H-stable, inert, non-toxic, temperature-resistant, and biodegradable polymer. In the present study, PVP capped silver nanoparticles are synthesized using glucose as a reducing agent, and studied the influence of PVP concentration on silver nanoparticles. Three different ratios of silver nitrate and PVP (1:1, 1:1.5, and 1:2) are taken for silver nanoparticle synthesis. Further, silver nanoparticles obtained are subjected to a series of examinations, including UV Spectrophotometry, SEM, X-Ray Diffraction Spectroscopy, Dynamic Light Scattering, and FTIR. The PVP capped silver nanoparticles are spherical, non-aggregated, polydisperse, and had a unimodal distribution, with diameters ranging from 40 to 100 nm. PVP capped silver nanoparticles are then subjected to antioxidant and antimicrobial activity investigation by spectrometry and agar well diffusion method respectively. The DPPH and the ABTS study revealed the radical scavenging activity of AgNPs. However, the PVP-capped silver nanoparticles did not show any antibacterial activity. This study showed the possibility of the application of PVP-capped AgNPs in the treatment of free radical-related diseases.

Statement
The study investigated the synthesis of silver nanoparticles (P-AgNPs) using a green method. We employed glucose as a reducing agent and PVP as a stabilizing agent. By varying the concentrations of AgNO3 and PVP to control the size, shape, and dispersity of the nanoparticles. Subsequently, the P-AgNPs were characterized using various techniques, and their antioxidant and antibacterial activities were evaluated.

Keywords Silver metal nanoparticle · PVP · Antioxidants · Anti-bacterial activity

1 Introduction

Nanoparticles (NPs) have size dimensions between approximately 1–100 nm [1]. Nanotechnology research has gained momentum for two decades substantially on account of the NP versatile physicochemical features such as temperature, thermal-electrical properties, catalytic behavior, and photo–activity [2]. Nanomaterials have a wide range of applications in agriculture, food, electronics, medicine, and textile industries [3]. Currently, metal nanoparticles (MNPs) with unprecedented properties are being extensively investigated due to their feasibility of application in various fields such as packing, coating, biological markers, and pharmaceutical industries [4, 5]. From a broad range of MNPs, silver nanoparticles (AgNPs) have enchanted intense research due to their peerless features such as excellent electrical

Extended author information available on the last page of the article

Published online: 08 August 2024

conductivity, catalysis, and a broad range of promising bioactivities including antioxidant, antibacterial, antifungal, anti-inflammatory, and anticancer effects [6]. The distinct physical, chemical, and biological properties of AgNPs are heavily influenced by factors such as size, morphology, as well as surface coating, which are generally controlled during nanoparticle synthesis [7]. As a result, proper synthesis method selection is critical for achieving the required properties for a specific application.

Synthesis of AgNPs is achieved through either physical, chemical, or green methods. However, due to problems associated with the consumption of a significant amount of energy, emission of poisonous and dangerous substances, usage of complicated equipment, and the synthesis conditions, physical and chemical methods are gradually being replaced by green synthesis methods [8]. In green synthesis, the reducing agent is obtained from natural and environmentally benign sources. The surface modification of AgNPs is done to prevent aggregation using a variety of capping and stabilizing agents, including surfactants like cetrimonium bromide (CTAB), polymers (like PVP), and green materials (like extracts of plant parts, such as tea leaves) [9]. To avoid NP agglomeration and reduce toxicity as well as to enhance the antibacterial effect, it is advantageous to reduce and cap silver metal complexes using green technology [10].

Capping agents such as halogens, citrate, and polymers are being employed to stabilise the NPs against aggregation in order to achieve the colloidal stability of AgNPs [11]. Since their addition frequently changes the form of NPs, it is believed that these capping agents play a dual role in synthesis, acting both as stabilising agents as well as structure directing agents (SDA) [12]. Among the wide range of capping materials, PVP is one that is water soluble, biocompatible, non-toxic, temperature- and *p*H-resistant, inert, and biodegradable polymer which is extensively used in nanoparticle synthesis because of its unique advantages [13]. To produce diverse shapes, such as cubes, octahedral, prisms, and wires, coinage metal NPs (Ag, Au, and Cu) are frequently synthesized using this method. Additionally, it is employed in the synthesis of numerous other MNPs, including lead, platinum, and ruthenium [12]. The irritability or toxicity of numerous medications, such as oxytetracycline, oxymetazoline, iodine, nicotine, cyanide, formaldehyde, and formamide, as well as toxins, is decreased due to their complexity. Because of its robust attachment to AgNP's surface, it offers greater stability than citrate or phenol [14]. In addition to these applications, it can serve as a delivery system for drugs as well as a carrier of AgNPs in nanocomposites that include silver. Due to the ability to regulate the quantity of released silver ions, which varies depending on the material loaded on AgNPs, silver-loaded Nano complexes demonstrated significant antibacterial activity and minimal toxicity [15]. Coated AgNPs with PVP (P-AgNPs) offer excellent structure functionalities, highly regularized pores, ordered crystalline structures, large surface areas, and a variety of other possible applications, including the purification of potable drinking water and the use in the food industry as packaging and color indicators [16].

Previous research has shown that P-AgNPs may is produced using $NaBH_4$ [17], PVP by self-reducing [18], citrate [19], plant extract [20], and other reductants. The conductivity of conductive ink has been tested using P-AgNPs reduced by glucose [21], but another study reported production of P-AgNPs with the help of a microwave [22]. The fact that numerous investigations have shown the impact of various reducing and stabilizing entities on the dimension, size distribution, and shape of P-AgNPs is particularly intriguing. Despite this, information on the aggregation behavior of NP is mostly absent from the scholarly literature. Specifically, particle aggregation has effects on several bioactive characteristics of the resulting nanomaterial. Generating non-toxicAgNPs for drug delivery systems is the primary objective of this study. The present study focuses on P-AgNPs that have been reduced by glucose and examines the impact of the concentration of PVP during the green synthesis process on the scale, optical characteristics, antioxidant properties, and antibacterial action.

2 Materials and Methods

2.1 Resources and Procedures

Silver nitrate (99.9% $AgNO_3$), glucose (M.W. 180), and polyvinylpyrrolidone (M.W. 1.3×10^5) were acquired from Merck (India). The solutions were made using Milli-Q water and all the compounds were used without additional purification.

2.2 Silver Nanoparticle Synthesis

The synthesis of P-AgNPs involved the green process that Chen et al., had previously described [21]. Silver nitrate was used as a source of silver, glucose as a reducing agent, PVP as a capping agent, and KOH to keep the *p*H of the solution alkaline. To maintain a 1:1 ratio of $AgNO_3$ and PVP, the synthesis of AgNPs was standardized using various concentrations of $AgNO_3$ (3, 5, 10, 15, and 20mM), glucose, and KOH (10mM). For further assessing the impact of various PVP concentrations on the morphology of AgNPs, the greatest peak obtained in the UV-Vis spectra with the aforementioned concentration was taken.

2.3 Characterization of Silver Nanoparticle

P-AgNPs were synthesized using PVP and Glucose. The formation of P-AgNPs was indicated by a colour change from white to colloidal dark brown and grey. Analysis of the AgNPs' by UV-Vis spectroscopy provides information about their synthesis and stability. The UV-Vis spectrophotometer (Shimadzu UV-1800) was used to measure the formation of the AgNPs in the 350–700 nm wavelength range [23]. To understand the successful capping and reduction of P-AgNPs, the FTIR spectrum was recorded in the region of 500–4000 cm^{-1} using the potassium bromide pellet method [24]. Using SEM (ZEISS EVO 15 with a 5 kV acceleration voltage), the shape and distribution of P-AgNPs were obtained [25]. The EDX device revealed the elemental composition of the formed P-AgNPs(Oxford -Aztec). With the help of an XRD instrument (Empyrean 3rd generation, Malvern PANanalytical) operating at 40 KV with a current of 30 mA and Co-Kα radiation, the structural phase present in P-AgNPs was identified. The crystalline size was then calculated using the Debye-Scherrer equation. The surface charge and size distribution were performed using DLS (3 LitessizerTM 500 and M/s Anton-Paar) instrument to comprehend them.

2.4 Antioxidant Activity

2.4.1 The 2,2-Diphenyl-1-Picrylhydrazyl (DPPH) Assay

DPPH assay was performed following Hulikere et al., for three distinct P-AgNPs, and standard quercetin [26]. The DPPH test's fundamental component is the stable DPPH free radical's propensity for reacting with hydrogen donors. Quercetin was used as a standard and 0.1mL of various sample concentrations (20, 40, 60, 80, and 100 µg/mL) were added to 150µL of the reagent (2mM DPPH), which was then incubated for 15 min. Methanol was employed as a blank solution, and DPPH served as the control. The absorbance was recorded at 517 nm using Bio-Rad's micro-plate reader(iMark). Using Eq. 1, the free radical scavenging activity was calculated.

2.4.2 The 2,2-Azino-Bis (3Ethylbenzothiazoline-6-Sulphonic acid) (ABTS) Assay

ABTS free radical scavenging assay of three distinct P-AgNPs, and standard ascorbic acid was performed following Hulikere et al. [26]. It is the most popular assay for figuring out free radical concentrations. This method is based on the neutralization of a radical cation that results from the one-electron oxidation of the synthetic chromophore ABTS. Ascorbic acid was used as a standard and 0.1mL of various sample concentrations (20, 40, 60, 80, and 100 µg/mL) were added to 150µL of the reagent (7mM ABTS and 4.95mM potassium permanganate) and incubated for 15 min. Water served as the blank solution, while ABTS served as the control. The absorbance was recorded at 740 nm using Bio-Rad's microplate reader. Using the formula below, the free radical scavenging activity was calculated.

$$\%Scavenging = \frac{Ac - As}{Ac} \quad (1)$$

where as represents the sample's absorbance and Ac represents the control's absorbance.

2.5 Antibacterial Activity of Silver Nanoparticle

P-AgNPs were tested for their antibacterial effectiveness against a variety of pathogenic strains that cause acquired infections, including *Escherichia coli, Bacillus subtilis, Staphylococcus aureus*, and *Pseudomonas aeruginosa*. The bacteria were grown on nutrient agar, and they were then kept at 37 °C for 24 h. A colony of bacteria was chosen and suspended in 5mL of nutritional broth using a sterile inoculating loop. To meet the 0.5 McFarland criteria, the turbidity of the bacterial suspension was modified. By streaking the swabs across the plates of nutrient agar, bacteria were inoculated. We used the well-diffusion method to conduct the antimicrobial test [27, 28]. The wells (5 mm in diameter) were made in each Petri plate using a cork borer, and 100µL of various concentrations (10, 25, 50, 100 µg) of P-AgNPs were placed in each well for the antibacterial test. A concentration of standard streptomycin and water at a concentration of 25 µg/mL was also used as a positive and negative control respectively. An inhibition against the microbiological species was noted in the zone of inhibition (in mm).

2.6 Statistical Evaluation

The mean and standard deviation of three independent data were used to express all experimental outcomes. Analysis of variance (ANOVA) was used in the statistical analysis of the data, which was carried out using the Origin 8.0 package.

3 Results and Discussion

The reduction of Ag ions (Ag) to P-AgNPs was carried out in an aqueous solution of PVP and dextrose in an alkaline medium, and the process was observed by visual inspection. Due to their small size, the initial reduction of silver ions was confirmed by the shift in color from colorless to distinctive yellow. The UV-Vis absorption spectrum demonstrated

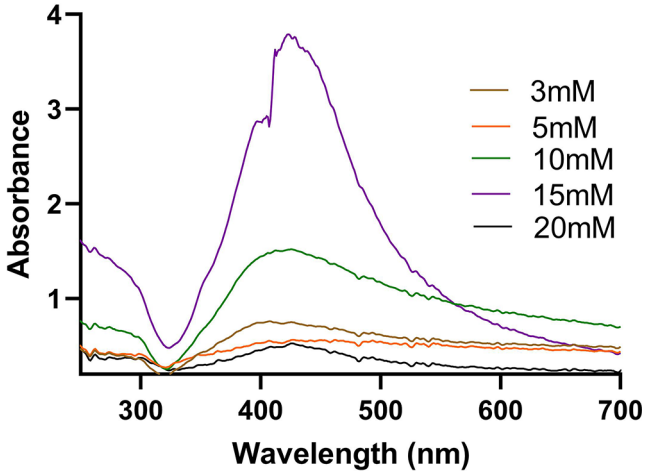

Fig. 1 Ultraviolet-visible spectra of P-AgNPs synthesized using 1:1 ratio of $AgNO_3$ and PVP. The Ultraviolet-visible spectra was studied at 3, 5, 10, 15, and 20 mM concentration of $AgNO_3$ and PVP in 1:1 ratio

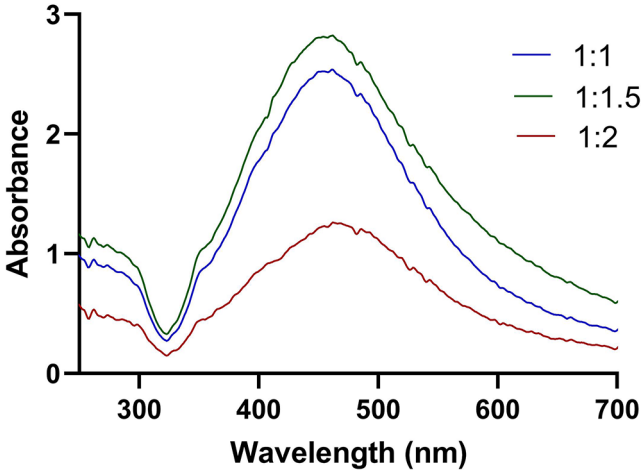

Fig. 2 Effect of different concentration (1, 1.5, and 2) of PVP at constant $AgNO_3$

an absorbance peak at 451 nm as a result of the excitation of small-sized P-AgNPs (supplementary Fig. 1) whereas $AgNO_3$ solution displayed a prominent peak in its UV-Vis spectra at 300 nm, when it splits into Ag^+ and NO_3^- ions [17]. The excitation of electrons on the surface of P-AgNPs in a particular electronic vibration mode also validated the size and shape of the particles. Noble MNPs have characteristic absorption spectra in the visible region as a result, which are easily detectable by a spectrophotometer [29].

3.1 The Effect of $AgNO_3$ Concentration on Silver Nanoparticles

During the synthesis of P-AgNPs, the impact of $AgNO_3$ concentration was examined. Different concentrations of $AgNO_3$ solution (3, 5, 10, 15, and 20 mM) were utilized. The absorbance in the UV-Vis spectrum increased with the increment in $AgNO_3$ concentration (3-15mM). However, the absorption peak reduced with a further increase in the concentration of $AgNO_3$ to 20 mM (Fig. 1). The probable reason for the decrease in absorbance beyond 15mM of $AgNO_3$ may be the too-high concentration. At higher concentrations, $AgNO_3$ can elevate solution ionic strength, diminishing repulsive electrostatic forces between AgNPs and enhancing attractive van der Waals forces, potentially increasing inter-nuclear collisions and agglomeration. In proximity, AgNPs may undergo coalescence, combining smaller particles into larger ones when the energy needed to overcome repulsion is surpassed by attractive forces. Under circumstances of insufficient stabilizer coverage or high precursor concentrations, the balance between nucleation and agglomeration may shift towards the latter, leading to fewer, larger particles instead of numerous, dispersed ones [30, 31].

3.2 Effect of PVP Concentration on Silver Nanoparticles

In Fig. 2 shows the UV-Vis spectra of the P-AgNPs that were produced with various $AgNO_3$ and PVP ratio. A strong and narrow Plasmon resonance band was observed at 445 nm for P-AgNPs synthesized using 1:1 and 1:1.5 ($AgNO_3$ and PVP) ratio, in contrast to 1:2 ratio which showed very broad peaks and wide size distribution. P-AgNPs with a 1:2 ratio resulted in a minor shift of the major absorption peak position towards a longer wavelength. AgNPs' surface is heavily covered with PVP, which may be the cause of the decrease in absorption intensity. The impact of PVP on AgNPs is evidenced through EDX data, which illustrates that at lower PVP concentrations, the metal constitutes 65.4%, while at slightly higher concentrations, it comprises 72.51% of the composition. With a further increase in PVP concentration, the metal content returns to 65.4%. Of all the SEM images, the 1:1 and 1:2 ratio P-AgNPs exhibited poor monodispersion and morphology in comparison to the 1:1.5 ratio. Triangle-shaped NPs were also present in a 1:2 ratio and this may be a result of the PVP being reduced under the reaction conditions. The above results confirm that PVP is crucial in determining the size, shape, monodisperse characteristics, and purity of P-AgNPs.

Regarding the mechanism of action that is concerned, PVP may functions as a stabilizer and surface-protecting agent during the synthesis of P-AgNPs. The silver crystal nuclei generated in the solution cannot be entirely encapsulated when PVP is present in minimal amounts. As a result, the majority of synthesized NPs are unable to develop into a typical spherical shape. Additionally, the partial aggregation is caused by the weaker electrostatic repulsion forces that exist between the NPs due to their inadequate wrapping. The silver crystal nuclei fully coated with PVP are

more likely to grow into a spherical shape even when the amount of PVP is adequate [32]. While doing so, the negatively charged amide strong polar groups of PVP enhance the electrostatic attraction between NPs. Therefore, it is advantageous to synthesize the spherical P-AgNPs with good dispersibility [15].

3.3 Scanning Electron Microscopy

SEM picture of P-AgNPswere shown in Fig. 3. The majority of the 1:1 ($AgNO_3$ and PVP) P-AgNPs were spherical in shape, with few being irregularly shaped, polydispersed, and showing a wide range of particles between 50 nm and 100 nm with a unimodal distribution. The average particle size was 74.92 nm. A low PVP concentration led to incomplete coverage of silver particles by PVP, causing agglomeration, broad polydisperse and uneven form. Additionally, the P-AgNPs synthesized of 1:1.5 ($AgNO_3$ and PVP) displayed spherical form, non-aggregated, polydisperse, and unimodal distribution with diameters of 40–80 nm this is possibly due to full PVP coating preventing agglomeration. The average particle size was 61.02 nm. NPs found to have a correct spherical form and narrow polydispersity. P-AgNPs with 1:2 ($AgNO_3$ and PVP) displayed spherical, triangular, and hexagonal shapes, non-aggregated, polydispersity with a unimodal distribution, and diameters between 50 and 100 nm. The P-AgNPs exhibited a slightly greater mean diameter while maintaining a narrow distribution (50 to 100 nm), implying that excessive PVP didn't enhance surface coverage. Elevating PVP concentration increased silver particle nucleation rate and decreased size until an optimum was reached at 1:1.5, suggesting that PVP could hinder aggregation and promote smaller nanoparticle formation. The concentration of capping molecules, as illustrated, significantly influences the control of mean diameter and particle size distribution in these P-AgNPs [33]. The average particle size was approximately 68.62 nm. Due to the abundance of PVP in this reaction, there may be potential for PVP to undergo self-reduction, which has led to the synthesis of NPs with various shapes, including triangle and hexagonal shapes. The 1:1.5 ($AgNO_3$ and PVP) P-AgNPs showed the narrowest particle size dispersion among the three distinct $AgNO_3$ and PVP preparation ratio. It is worth noting that with PVP, the average size of the NPs formed decreased when compared to 1:1 and 1:2 ratio. From the SEM pictures, it was also clear that 1:1.5 ($AgNO_3$ and PVP) P-AgNPs resulted in a reduction in polydispersity and mean particle size. This may be because of the PVP's increased ability to donate electrons which causes it to engage with positively charged silver ions more forcefully during reduction. Consequently, there is improved stability between the capping molecule and the AgNPs surface. Chen *et al.,*. found that the average size of AgNPs made from glucose was 88 nm, which was greater than hydrazine hydrate (38 nm) [21]. It is in agreement with our results.

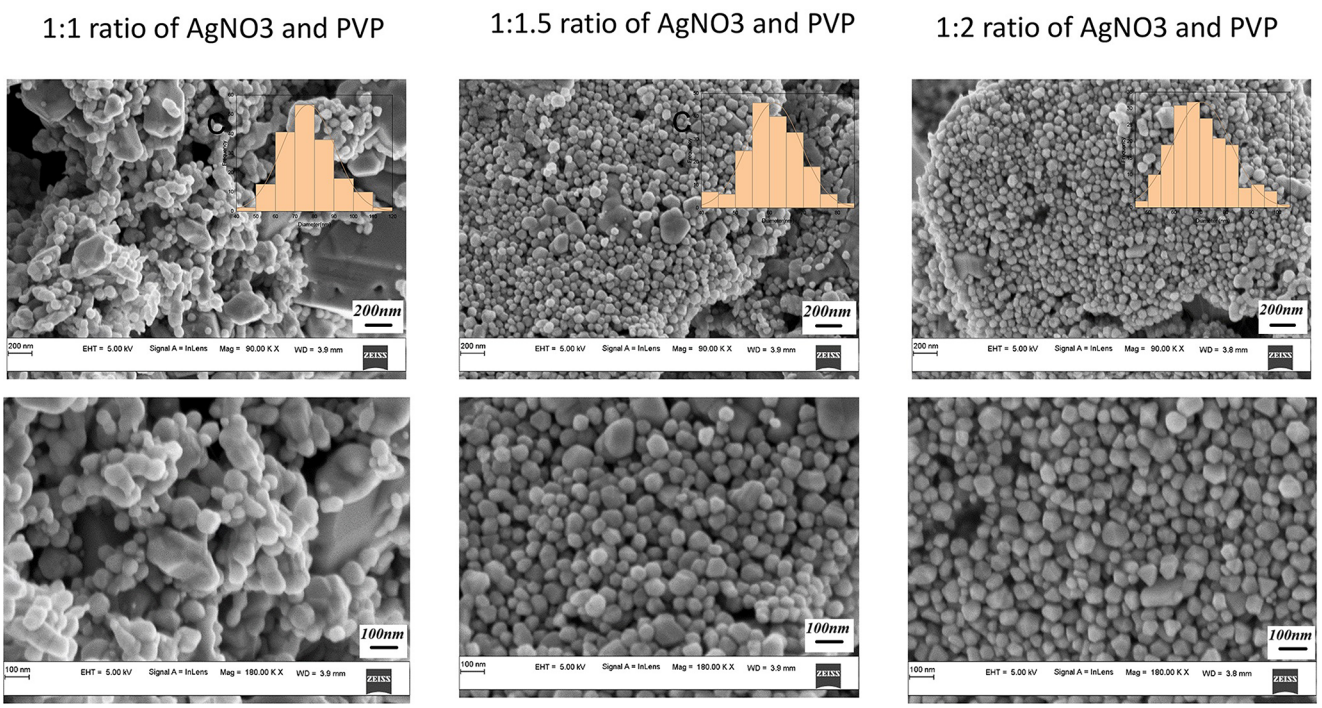

Fig. 3 Scanning electron microscope images of P-AgNPs synthesized using 1:1, 1:1.5, and 1:2 ratios of $AgNO_3$ and PVP

3.4 Dynamic Light Scattering

Dynamic light scattering (DLS), as illustrated in supplementary Fig. 2, was used to measure the average hydrodynamic size (HDS) and polydispersity index (PDI) of the three distinct P-AgNPs in an aqueous buffer. 1:1 ($AgNO_3$ and PVP) P-AgNPs had has an average particle size of 214.7 nm and a PDI of 0.198, whereas 1:1.5 ($AgNO_3$ and PVP) P-AgNPs had an average size of 219.6 nm and a PDI of 0.16. However, the P-AgNPs of 1:2 ($AgNO_3$ and PVP) showed that their average particle size is 207.5 nm and their PDI was 0.143. The probable effects of PVP as a stabilizing agent and glucose as a reductant are responsible for the variations in particle size for the three samples. The results indicates that the elevation in HDS from 214.7 nm to 219.6 nm could potentially be linked to an augmentation in the silver's percentage composition, resulting in an intensified electrostatic force. Moreover, the decrease in HDS from 219.6 nm to 207.5 nm might be attributed to the substantial non-ionic PVP coverage potentially diminishing the electrostatic force and became well dispersed with increasing PVP concentration. The hydrodynamic diameter of the P-AgNPs is impacted by the presence of PVP as a capping agent, which surrounds and creates a layer around the AgNPs [14].

3.5 Surface Properties and Stability (EDX, FTIR, ZP, XRD)

3.5.1 Energy Dispersive Spectrum Analysis

The EDX examination of the reduced P-AgNPs revealed a peak in the optical absorption characteristics at 3 keV (supplementary Fig. 3). The EDX examination of the 1:1 and 1:2 ($AgNO_3$ and PVP) P-AgNPs revealed the same relative percentage composition of elements, such as oxygen (O) at 23.11%, carbon (C) at 11.50%, and silver (Ag) at 65.49%. While the oxygen (O) content of 1:1.5 ($AgNO_3$ and PVP) P-AgNPs was 18.33%, the carbon (C) content was 9.16%, and the silver (Ag) content was 72.51%. The carbon and oxygen molecules acted as organic capping agents attached to the surface of P-AgNPs. The peak corresponding to carbon and oxygen may be due to the presence of PVP and glucose. Out of all three P-AgNPs, 1:1.5 ($AgNO_3$ and PVP) showed the highest percentage of silver (Ag) element.

3.6 X-Ray Diffraction Analysis

In Fig. 4 displays the stabilized three distinct P-AgNPs' XRD pattern. The (111), (200), (220), (311), and (222) planes of the face-centered cubic (fcc) crystal structure of metallic silver were represented by five clearly defined distinctive diffraction peaks at 38.3°, 44.5°, 64.8°, 77.6°, and 81.8°, respectively. P-AgNPs' XRD spectrum yielded interplanar spacing (d_{hkl}) values of 2.307, 2.012, 1.437, 1.229, and 1.176 and a lattice constant (4.047) that correspond with the values for standard silver (JCPDS PDF card 04-0783).

3.7 Zeta Potential

The average zeta potential of the synthesised P-AgNPs with 1:1, 1:1.5, and 1:2 ($AgNO_3$ and PVP) was correspondingly -13.1 ± 0.6mV, -16.1 ± 0.6mV, and -06.7 ± 0.4mV (supplementary Fig. 4). The zeta potential of the 1:1.5 ($AgNO_3$ and PVP) P-AgNPs showed a larger average value but the difference between -13.1 and -16.1 is not a vast difference when compared to -6.7. The stability depends on various factors, such as repulsive forces of P-AgNPs [34], interaction between PVP and glucose molecules on the P-AgNPs surface, *p*H of the solution [35] leading to alterations in the surface charge and consequently affecting zeta potential.

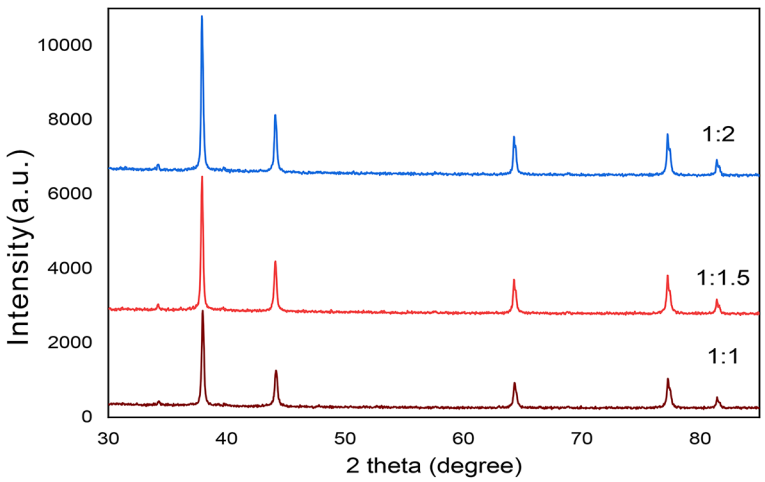

Fig. 4 Powder X-ray Diffraction spectra of P-AgNPs synthesized using 1:1, 1:1.5, and 1:2 ratios of $AgNO_3$ and PVP

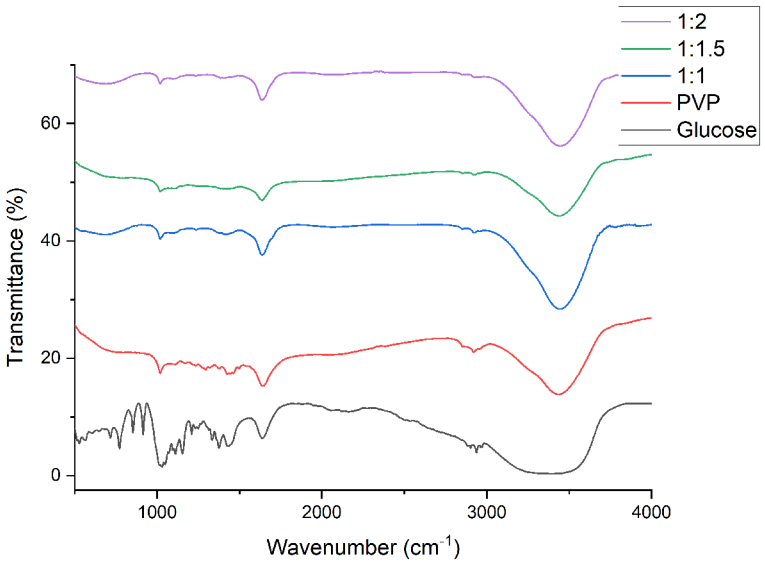

Fig. 5 Fourier-transform infrared spectra of PVP, Glucose and P-AgNPs synthesized using 1:1, 1:1.5, and 1:2 ratios of $AgNO_3$ and PVP

Table 1 Mean value of DPPH and ABTS radical scavenging activity of standard, and different ratio of $AgNO_3$ and PVP (1:1, 1:1.5, 1:2) of P-AgNP

	DPPH	ABTS
Standard	85.15 ± 0.70	84.07 ± 0.85
1:1	36.5 ± 0.25	31.47 ± 0.33
1:1.5	41.1 ± 0.56	31.2 ± 0.41
1:2	37.8 ± 0.34	33.17 ± 0.27

3.8 Fourier Transform Infrared Spectroscopy (FTIR)

FTIR was used to pinpoint the functional groups that were in charge of the reduction of Ag^+ and capping of synthesized P-AgNPs. Figure 5 displays the FTIR spectra of glucose, PVP, and various P-AgNPs in the frequency range of 4000–500 cm^{-1}. A strong peak at 3400 cm^{-1} in the spectra indicates an N-H stretch with an amide group. The C-H stretch containing alkene groups is observed at 2922 cm^{-1}. Bond vibrations of the N-H-O complex and NO_3 group are reported to have peaks at 1234 and 1384 cm^{-1}, respectively. The presence of PVP, which is inhibiting further development and agglomeration, is shown by the resonance peak at 1638 cm^{-1}, which is caused by the C = O group stretching of PVP. The presence of a functional C-N unit is indicated by the stretching vibration peak at 1018 cm^{-1}, which is both asymmetric and symmetric. A strong absorption band and carbonyl stretch cause the band at 766 cm^{-1} to deform.

3.9 Antioxidant Activity

This study set out to evaluate how well P-AgNPs performed as antioxidants when they were encapsulated in varied PVP concentrations because AgNPs are already known to possess antioxidant properties. By using the DPPH and ABTS techniques, the anti-oxidant activity was evaluated.

Table 1 illustrates the proportion of radical scavenging for P-AgNPs at various concentrations. The P-AgNPs have less antioxidant activity. This is because AgNPs are covered in a protective coating of PVP. The DPPH scavenging activity of P-AgNPs of 1:1, 1:1.5, and 1:2 ($AgNO_3$ and PVP) were found to be 36.5 ± 0.25, 41.1 ± 0.56, and 37.8 ± 0.34% respectively. ABTS scavenging activity of P-AgNPs of 1:1, 1:1.5, and 1:2 ($AgNO_3$ and PVP) showed 31.47 ± 0.33, 31.2 ± 0.41, and 33.1 ± 0.27% scavenging respectively. This variation in antioxidant activity can be attributed to the differences in the PVP concentration, which affects the surface coverage of nanoparticles and subsequently influences their interaction with the antioxidant radicals. As the PVP concentration increases, the stability and coverage of nanoparticles may improve, leading to better interaction with DPPH and ABTS radicals. From the above results, there is not much difference between the three distinct P-AgNPs. Despite PVP shielding, AgNPs showed strong antioxidant activity compared to non-cytotoxic silver nanoparticles synthesized using apple pulp and cumin seed extracts developled by Jahan *et al.,*. The highest concentration of cumin seed AgNPs exhibited 27.84% DPPH scavenging, while apple pulp AgNPs showed 13.12% [36].

3.10 Antibacterial Activity

The agar well diffusion method was used to investigate AgNPs' antibacterial activity against Gram-positive and Gram-negative species (supplementary Fig. 5). Table 2 provides the maximal diameter of the inhibitory zone for various AgNP concentrations. AgNPs with PVP caps has been demonstrated to have no antibacterial activity. This outcome is at odds with earlier research that examines the antibacterial abilities of AgNPs capped with PVP [37]. The

Table 2 Antibacterial activity of different ratio of $AgNO_3$ and PVP (1:1, 1:1.5, 1:2) of P-AgNP, Control, and Standard

Test organism	Inhibition zone in mm by 1:1	Inhibition zone in mm by 1:1.5	Inhibition zone in mm by 1:2	Control (dist.water)	Standard (Streptomycin)
E.coli	-	-	-	-	1.6 cm
B.subtilis	-	-	-	-	1.3 cm
S.aureus	-	-	-	-	1 cm
P. auriginosa	-	-	-	-	1.1 cm

development of a PVP layer surrounding AgNPs blocks the release of silver ions which will result in the lack of antibacterial activity [30]. However, by altering the environment, it is possible to boost the antibacterial activity of PVP-AgNPs by making the PVP more soluble and, in turn, controlling the number of released ions. On the other hand, the lack of antibacterial action of PVP-AgNPs is consistent with earlier research by Zein *et al.,*. By conjugating AgNPs with several antibiotic classes, they increased the bactericidal efficacy [38–41]. Whereas the synergistic impact is attributed to the drug-AgNPs conjugates which accelerate the release of silver ions [15, 42].

4 Conclusion

A low-cost, environmentally friendly, and green method was used to synthesize P-AgNPs. The structure, size, and stability of P-AgNPs will unquestionably be impacted by the minimum and maximum amounts of PVP used as a capping agent. The P-AgNPs of 1:1.5 showed better size, shape, and stability compared to 1:1 and 1:2 P-AgNPs. Even though it is covered with PVP, P-AgNPs showed antioxidant activity. Although it was checked for only 4 types of bacteria and none showed an antibacterial effect. This finding opens up new possibilities for controlling AgNP size and colloidal stability using PVP these unique property of P-AgNPs could be exploited further for the treatment of radical related disease such as cancer and neurological disorder. Finally, research on conjugating these non-toxic PVP-AgNPs to medicines or natural compounds as a drug delivery system needs to be developed for the future.

Supplementary Information The online version contains supplementary material available at https://doi.org/10.1007/s40010-024-00882-y.

Acknowledgements The authors are thankful to Mangalore University for its support. The authors are thankful to DST-PURSE and NITK-Surathkal for the sample analysis. All authors thank the Principal of Alva's Ayurveda Medical College, the Director of ATMA Research Center, and the Management of Alva's Education Foundation (AEF), Vidyagiri, Moodubidire for their continuous support and encouragement.

Author Contributions Dinesh B: Investigation, formal analysis, data curation, writingoriginal draft, writing- review and editing, project administration and funding acquisition. Jagadeesha Poyya: Software, validation, formal analysis, data curation, writing-review and editing. Farhan Zameer: Formal analysis, data curation, writing- review and editing. Lokesh Koodlur Sannegowda: writing-review and editing. Chandrashekhar G. Joshi: Conceptualization, methodology, investigation, validation, formal analysis, data curation, resources, writing-review and editing, supervision and funding acquisition. Anjanapura V. Raghu: data curation, writing-review and editing. All authors have read and approved the manuscript.

Data Availability The data relevant to the findings of the study are available from the corresponding author upon reasonable request.

Declarations

Conflict of Interest The authors declare no conflicts of interest.

References

1. Dinesh B, Monisha N, Shalini HR et al (2022) Antibacterial activity of silver nanoparticles synthesized using endophytic fungus—*penicillium cinnamopurpureum*. Spectrosc Lett 55:20–34. https://doi.org/10.1080/00387010.2021.2010764
2. Salata O (2004) Applications of nanoparticles in biology and medicine. J Nanobiotechnol 2:3. https://doi.org/10.1186/1477-3155-2-3
3. Pandey G, Jain P (2020) Assessing the nanotechnology on the grounds of costs, benefits, and risks. Beni-Suef Univ J Basic Appl Sci 9:63. https://doi.org/10.1186/s43088-020-00085-5
4. Kannan K, Radhika D, Reddy KR et al (2021) Gd3 + and Y3 + co-doped mixed metal oxide nanohybrids for photocatalytic and antibacterial applications. Nano Ex 2:010014. https://doi.org/10.1088/2632-959X/abdd87
5. He Y, Wei F, Ma Z et al (2017) Green synthesis of silver nanoparticles using seed extract of Alpinia katsumadai, and their antioxidant, cytotoxicity, and antibacterial activities. RSC Adv 7:39842–39851. https://doi.org/10.1039/c7ra05286c
6. Ying S, Guan Z, Ofoegbu PC et al (2022) Green synthesis of nanoparticles: current developments and limitations. Environ Technol Innov 26:102336. https://doi.org/10.1016/j.eti.2022.102336
7. Zhang X-F, Liu Z-G, Shen W, Gurunathan S (2016) Silver nanoparticles: synthesis, characterization, properties, applications, and therapeutic approaches. Int J Mol Sci 17:1534
8. Dinesh B, Chethan MU, Pratap GK et al (2021) Biogenic synthesis of silver nanoparticles using *Aspergillus Aureoles* (Endophyte) and demonstration of their Anti- microbial activity. Anal Chem Lett 11:899–910. https://doi.org/10.1080/22297928.2021.2007789
9. Rónavári A, Bélteky P, Boka E et al (2021) Polyvinyl-pyrrolidone-coated silver nanoparticles—the Colloidal, Chemical, and

Biological consequences of Steric Stabilization under Biorelevant conditions. Int J Mol Sci 22:8673. https://doi.org/10.3390/ijms22168673
10. Chugh D, Viswamalya VS, Das B (2021) Green synthesis of silver nanoparticles with algae and the importance of capping agents in the process. J Genet Eng Biotechnol 19:126. https://doi.org/10.1186/s43141-021-00228-w
11. Bassous NJ, Webster TJ (2020) Metal- and polymer-based nanoparticles for Advanced Therapeutic and Diagnostic System Applications. In: Li B, Moriarty TF, Webster T, Xing M (eds) Racing for the Surface: Pathogenesis of Implant infection and advanced antimicrobial strategies. Springer International Publishing, Cham, pp 357–384
12. Chen Z, Chang JW, Balasanthiran C et al (2019) Anisotropic growth of silver nanoparticles is kinetically controlled by polyvinylpyrrolidone binding. J Am Chem Soc 141:4328–4337. https://doi.org/10.1021/jacs.8b11295
13. Kurakula M, Rao GSNK (2020) Pharmaceutical assessment of polyvinylpyrrolidone (PVP): as excipient from conventional to controlled delivery systems with a spotlight on COVID-19 inhibition. J Drug Deliv Sci Technol 60:102046. https://doi.org/10.1016/j.jddst.2020.102046
14. Kamarudin D, Hashim NA, Ong BH et al (2022) Synthesis of silver nanoparticles stabilised by PVP for polymeric membrane application: a comparative study. Mater Technol 37:289–301. https://doi.org/10.1080/10667857.2021.1908768
15. Zein R, Alghoraibi I, Soukkarieh C et al (2022) Influence of Polyvinylpyrrolidone Concentration on properties and anti-bacterial activity of Green Synthesized Silver nanoparticles. Micromachines 13:777. https://doi.org/10.3390/mi13050777
16. Kumar A, Choudhary A, Kaur H et al (2021) Metal-based nanoparticles, sensors, and their multifaceted application in food packaging. J Nanobiotechnol 19:256. https://doi.org/10.1186/s12951-021-00996-0
17. Mirzaei A, Janghorban K, Hashemi B et al (2017) Characterization and optical studies of PVP-capped silver nanoparticles. J Nanostructure Chem 7:37–46. https://doi.org/10.1007/s40097-016-0212-3
18. Koczkur KM, Mourdikoudis S, Polavarapu L, Skrabalak SE (2015) Polyvinylpyrrolidone (PVP) in nanoparticle synthesis. Dalton Trans 44:17883–17905. https://doi.org/10.1039/C5DT02964C
19. Oprica L, Andries M, Sacarescu L et al (2020) Citrate-silver nanoparticles and their impact on some environmental beneficial fungi. Saudi J Biol Sci 27:3365–3375. https://doi.org/10.1016/j.sjbs.2020.09.004
20. Manjunath Hulikere M, Joshi CG (2019) Characterization, antioxidant and antimicrobial activity of silver nanoparticles synthesized using marine endophytic fungus- Cladosporium cladosporioides. Process Biochem 82:199–204. https://doi.org/10.1016/j.procbio.2019.04.011
21. Chen Q, Liu G, Chen G et al (2017) Green synthesis of silver nanoparticles with glucose for conductivity enhancement of conductive ink. BioResources 12:608–621
22. Seku K, Kishore Kumar K, Narasimha G, Bhagavanth Reddy G (2022) Chap. 7 - bio-mediated synthesis of silver nanoparticles via microwave-assisted technique and their biological applications. In: Abd-Elsalam KA (ed) Green Synthesis of Silver Nanomaterials. Elsevier, pp 149–188
23. Danagoudar A, Pratap GK, Shantaram M et al (2020) Characterization, cytotoxic and antioxidant potential of silver nanoparticles biosynthesised using endophytic fungus (Penicillium Citrinum CGJ-C1). Mater Today Commun 25:101385
24. K C, SM SSG, S. K (2020) A FTIR approach of green synthesized silver nanoparticles by Ocimum sanctum and Ocimum gratissimum on mung bean seeds. Inorg Nano-Metal Chem 50:606–612. https://doi.org/10.1080/24701556.2020.1723025
25. Rautela A, Rani J, Debnath M (2019) Green synthesis of silver nanoparticles from Tectona grandis seeds extract: characterization and mechanism of antimicrobial action on different microorganisms. J Anal Sci Technol 10:5. https://doi.org/10.1186/s40543-018-0163-z
26. Hulikere MM, Joshi CG, Ananda D, Nivya T (2016) Antiangiogenic, wound healing and antioxidant activity of Cladosporium cladosporioides (endophytic fungus) isolated from seaweed (Sargassum Wightii). Mycology 7:203–211. https://doi.org/10.1080/21501203.2016.1263688
27. Joshi MMH, Danagoudar CG A, et al (2017) Biogenic synthesis of gold nanoparticles by marine endophytic fungus-Cladosporium cladosporioides isolated from seaweed and evaluation of their antioxidant and antimicrobial properties. Process Biochem 63:137–144. https://doi.org/10.1016/j.procbio.2017.09.008
28. Chougale R, Kasai D, Nayak S et al (2020) Design of ecofriendly PVA/TiO2-based nanocomposites and their antifungal activity study. Green Mater 8:40–48. https://doi.org/10.1680/jgrma.19.00002
29. Ider M, Abderrafi K, Eddahbi A et al (2017) Silver metallic nanoparticles with Surface Plasmon Resonance: synthesis and characterizations. J Clust Sci 28:1051–1069. https://doi.org/10.1007/s10876-016-1080-1
30. Gharibshahi L, Saion E, Gharibshahi E et al (2017) Influence of poly(vinylpyrrolidone) concentration on properties of silver nanoparticles manufactured by modified thermal treatment method. PLoS ONE 12:e0186094. https://doi.org/10.1371/journal.pone.0186094
31. Thanh NTK, Maclean N, Mahiddine S (2014) Mechanisms of Nucleation and Growth of nanoparticles in Solution. Chem Rev 114:7610–7630. https://doi.org/10.1021/cr400544s
32. Liu G, Ma X, Sun X et al (2018) Controllable synthesis of silver nanoparticles using three-phase Flow pulsating mixing microfluidic chip. Adv Mater Sci Eng 2018:1–14. https://doi.org/10.1155/2018/3758161
33. Dang TMD, Le TTT, Fribourg-Blanc E, Dang MC (2012) Influence of surfactant on the preparation of silver nanoparticles by polyol method. Adv Nat Sci NanoSci NanoTechnol 3:035004
34. Fen LB, Chen S, Kyo Y et al (2013) The Stability of Silver Nanoparticles in a model of pulmonary surfactant. Environ Sci Technol 47:11232–11240. https://doi.org/10.1021/es403377p
35. Kalliola S, Repo E, Sillanpää M et al (2016) The stability of green nanoparticles in increased pH and salinity for applications in oil spill-treatment. Colloids Surf a 493:99–107. https://doi.org/10.1016/j.colsurfa.2016.01.011
36. Jahan I, Erci F, Isildak I (2021) Rapid green synthesis of non-cytotoxic silver nanoparticles using aqueous extracts of Golden Delicious apple pulp and cumin seeds with antibacterial and antioxidant activity. SN Appl Sci 3:94. https://doi.org/10.1007/s42452-020-04046-6
37. Dey A, Dasgupta A, Kumar V et al (2015) Evaluation of the of antibacterial efficacy of polyvinylpyrrolidone (PVP) and trisodium citrate (TSC) silver nanoparticles. Int Nano Lett 5:223–230. https://doi.org/10.1007/s40089-015-0159-2
38. Mathew T, Sree RA, Aishwarya S et al (2020) Graphene-based functional nanomaterials for biomedical and bioanalysis applications. FlatChem 23:100184. https://doi.org/10.1016/j.flatc.2020.100184
39. Phyto-Nano-Antimicrobials: Synthesis, Characterization, Discovery, and Advances. In: https://www.eurekaselect.com. http://www.eurekaselect.com/chapter/14069. Accessed 2 Feb 2023
40. Patil AG, Kounaina K, Aishwarya S et al (2021) Myco-Nanotechnology for sustainable agriculture: challenges and

opportunities. Recent Trends Mycological Res 457–479. https://doi.org/10.1007/978-3-030-60659-6_20
41. Zabiulla, Al-Ostoot FH, Khamees HA et al (2022) In-silico docking, synthesis, structure analysis, DFT calculations, energy frameworks, and pharmacological intervention of [1,3,4]-thiadiazoles analogous as XO inhibitor and on multiple molecular inflammatory targets COX and LOX. J Mol Struct 1270:133963. https://doi.org/10.1016/j.molstruc.2022.133963
42. Prasad A, Baker S, Nagendra Prasad MN et al (2019) Phytogenic synthesis of silver nanobactericides for anti-biofilm activity against human pathogen H. Pylori. SN Appl Sci 1:341. https://doi.org/10.1007/s42452-019-0362-2

Authors and Affiliations

B. Dinesh[1] · Jagadeesha Poyya[1,2] · Farhan Zameer[3] · Lokesh Koodlur Sannegowda[4] · Chandrashekhar G. Joshi[1] · Anjanapura V. Raghu[5,6]

✉ Chandrashekhar G. Joshi
cgjoshi@mangaloreuniversity.ac.in

✉ Anjanapura V. Raghu
avraghu23@gmail.com

B. Dinesh
dinesh.bhaskar1993@gmail.com

Farhan Zameer
farhanzameeruom@gmail.com

[1] Department of Biochemistry, Mangalore University, Mangalore, Karnataka 583 105, India

[2] SDM Research Institute for Biomedical Sciences (SDMRIBS), Shri Dharmasthala Manjunatheshwara University, Dharwad, Karnataka 583 105, India

[3] Department of Dravyaguna (Ayurveda Pharmacology), PathoGutOmics Laboratory, Alva's Ayurveda Medical College, Alva's Traditional Medicine Archive (ATMA) Research Centre, Vidyagiri, Moodubidire, Dakshina Kannada - 574 227, Padavu, Karnataka, India

[4] Department of Studies in Chemistry, Vijayanagara Sri Krishnadevaraya University, Ballari, Karnataka 583 105, India

[5] Department of Basic Science, Faculty of Science & Technology, CMR University, Lakeside Campus, Bengaluru, Karnataka 562 149, India

[6] Faculty of Science and Technology, BLDE (Deemed-to-be University), Vijayapura, Karnataka 586109, India